

# Expected declines in recruitment of walleye pollock (*Theragra chalcogramma*) in the eastern Bering Sea under future climate change

Franz J. Mueter<sup>1\*</sup>, Nicholas A. Bond<sup>2</sup>, James N. Ianelli<sup>3</sup>, and Anne B. Hollowed<sup>3</sup>

<sup>1</sup>School of Fisheries and Ocean Sciences, University of Alaska Fairbanks, Juneau, AK 99801, USA

<sup>2</sup>Joint Institute for the Study of the Atmosphere and Oceans, University of Washington, Seattle, WA 98195, USA

<sup>3</sup>National Oceanic and Atmospheric Administration, National Marine Fisheries Service, Alaska Fisheries Science Center, 7600 Sand Point Way NE, Seattle, WA 98115, USA

\*Corresponding Author: tel: +1 907 796 5448; fax: +1 907 796 5446; e-mail: [fmuetter@alaska.edu](mailto:fmuetter@alaska.edu)

Mueter, F. J., Bond, N. A., Ianelli, J. N., and Hollowed, A. B. 2011. Expected declines in recruitment of walleye pollock (*Theragra chalcogramma*) in the eastern Bering Sea under future climate change. – ICES Journal of Marine Science, 68: 1284–1296.

Received 6 August 2010; accepted 14 January 2011; advance access publication 29 March 2011.

A statistical model is developed to link recruitment of eastern Bering Sea walleye pollock (*Theragra chalcogramma*) to variability in late summer sea surface temperatures and to the biomass of major predators. The model is based on recent advances in the understanding of pollock recruitment, which suggest that warm spring conditions enhance the survival of early larvae, but high temperatures in late summer and autumn are associated with poor feeding conditions for young-of-year pollock and reduced recruitment in the following year. A statistical downscaling approach is used to generate an ensemble of late summer temperature forecasts through 2050, based on a range of IPCC climate projections. These forecasts are used to simulate future recruitment within an age-structured stock projection model that accounts for density-dependent effects (stock–recruitment relationship), the estimated effects of temperature and predation, and associated uncertainties. On average, recruitment in 2040–2050 should be expected to decline by 32–58% relative to a random recruitment scenario, depending on assumptions about the temperature relationship, the magnitude of density-dependence, and future changes in predator biomass. The approach illustrated here can be used to evaluate the performance of different management strategies and provide long-term strategic advice to managers confronted with a rapidly changing climate.

**Keywords:** Bering Sea, climate change, forecasting, recruitment, sea surface temperature, statistical downscaling, walleye pollock.

## Introduction

Climate change will be expected to affect marine fish communities and fisheries production through a variety of direct and indirect effects of predicted changes in temperature, winds, salinity, stratification, oxygen, pH, and other factors (Brander, 2010). Climate-related changes have been documented in many ecosystems. Although the mechanisms are often uncertain, changes to recruitment success through changes in production or survival are believed to be the key process driving these changes (Rijnsdorp *et al.*, 2009). Forecasting the effects of climate change on a fish population requires (i) an understanding of the mechanisms linking climate drivers to fish production (recruitment, growth, and distribution), (ii) forecasts of the key climate drivers, and (iii) a stock projection model that captures the essential dynamics of the population of interest (Hollowed *et al.*, 2009). A critical requirement of this approach is that the known or presumed mechanisms affecting fish production can be quantified through robust statistical relationships and that these relationships remain valid under anticipated climate changes. Here the approach outlined by Hollowed *et al.* (2009) is illustrated with a case study by modelling the possible responses of walleye pollock in the eastern Bering Sea to future climate variability.

Walleye pollock are an important component of the eastern Bering Sea ecosystem and currently support the second largest single-species fishery in the world, with landings for the eastern Bering Sea alone ranging from 800 000 to 1.4 million tonnes over the past three decades. Their geographic range extends from Japan to the Bering Sea and as far south as northern California. In the eastern Bering Sea, walleye pollock occupy a central position in the foodweb and serve as a key forage species for many upper trophic level species, including fish, seabirds, and marine mammals (Aydin *et al.*, 2007). In addition, cannibalism is a major source of mortality for juvenile pollock. Adults consume primarily age-0 pollock during autumn and winter on the southeastern portion of the shelf and age-1 pollock during summer, autumn, and winter to the northwest of the Pribilof Islands (Dwyer *et al.*, 1987), consistent with the observed distribution of age-0 and age-1 pollock (Figure 1).

Spawning concentrations of walleye pollock in the eastern Bering Sea, as inferred from the distribution of eggs, occur near Bogoslof Island, north of Unimak Island and the Alaska Peninsula, and around the Pribilof Islands (Figure 1; Bachevalier *et al.*, 2010). Spawning takes place in February and March around Bogoslof, in March and April north of Unimak Island,

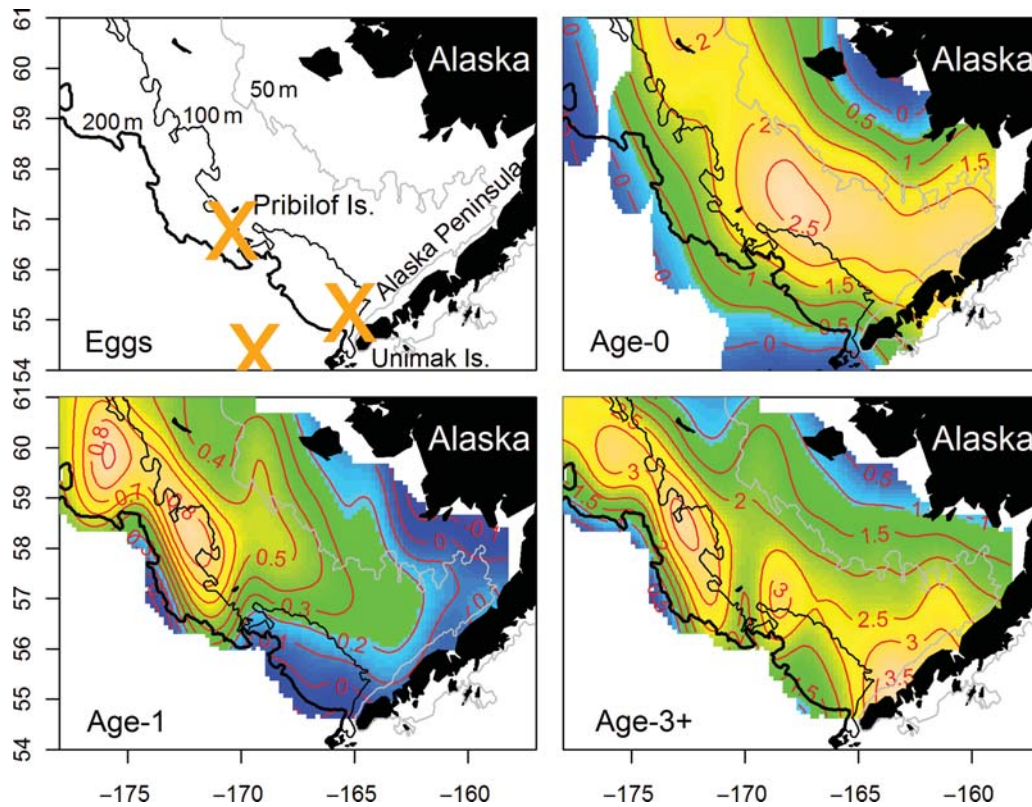


**Figure 1.** Distribution of pollock at various life stages, including main concentrations of eggs collected by NOAA's FOCI programme (Bacheler *et al.*, 2010), smoothed distribution of age-0 walleye pollock in autumn from Bering-Aleutian Salmon International Survey (BASIS) research programme, smoothed distribution of age-1 (80–199 mm), and age 3+ walleye pollock ( $\geq 300$  mm) during summer averaged over 1982–2009 NMFS bottom-trawl surveys.

and from April to August around the Pribilof Islands (Bacheler *et al.*, 2010). However, little spawning has been evident around Bogoslof Island in recent years, because of a very low spawning biomass (Ianelli *et al.*, 2009). By autumn of their first year, pollock are primarily distributed over the middle shelf, whereas age-1 pollock in the following summer primarily occupy the outer shelf to the northwest of the Pribilof Islands (Figure 1). Pollock also undertake northward and shoreward feeding migrations during spring and summer (Kotwicki *et al.*, 2005). Therefore, pollock utilize large portions of the middle and outer shelf; hence our efforts to identify environmental drivers of recruitment will focus on this area, in particular the middle-shelf region, which is important for age-0 pollock at a potentially critical stage in their early life (Hunt *et al.*, 2011).

Based on previous studies (as reviewed in Mueter *et al.*, 2006) and recent results from the Bering Sea Integrated Ecosystem Research Program (Hunt *et al.*, 2011), conditions affecting recruitment of walleye pollock include: (i) ice and temperature conditions at the time of hatching, which determine early feeding conditions; (ii) summer stratification over the shelf during the first summer (age 0), which affects feeding conditions of late larval stages, as well as vulnerability to predation; (iii) the abundance and distribution of potential predators, including predation of adult pollock, arrowtooth flounder, and other predators on age-0 and age-1 pollock. Moreover, the magnitude of predation may be affected by the spatial overlap between larval or juvenile pollock and their predators, including adult walleye pollock (Wyllie-Echeverria, 1996; Westgaard *et al.*, 2000; Mueter *et al.*, 2006).

Our current understanding of the drivers of walleye pollock recruitment in the eastern Bering Sea is based on a modified version of the oscillating control hypothesis (OCH) originally proposed by Hunt *et al.* (2002) and recently revised based on new findings (Hunt *et al.*, 2011). The OCH predicted that pollock recruitment should be greatest in warm years when ice retreats early and a late bloom occurs in thermally stratified water. These conditions favour the pelagic community, because primary production is consumed within the surface layer by zooplankton that serve as prey for larval walleye pollock. Although this prediction is supported by high survival of walleye pollock larvae from hatching to summer during the most recent warm period from 2002 to 2005, these years failed to produce large, lipid-rich zooplankton, such as *Calanus*, which provide important food for walleye pollock during late summer and autumn (Coyle *et al.*, 2011). Consequently, larval pollock during these warm years had low energy densities in autumn and may have experienced low overwinter survival, because of increased predation or starvation (Moss *et al.*, 2009). Therefore conditions in late summer and autumn may be critical to the overall survival of pollock from spawning to recruitment at age 1.

In this study, we build on these observations to develop an empirical relationship between late summer environmental conditions and walleye pollock survival from age 0 to age 1. This relationship is used within a simplified stock projection model to forecast recruitment of walleye pollock over the next 40 years. Our goal is to provide projections of future recruitment and abundance under different warming scenarios and under a plausible

harvest scenario. Major sources of uncertainty in climate projections and in the estimated environmental relationships are accounted for to characterize the full range of likely population trajectories under the selected harvest scenario. We first examine the empirical evidence of the proposed recruitment mechanisms to develop a robust functional relationship between recruitment of walleye pollock in the eastern Bering Sea and key climate variables. A statistical downscaling approach is then used to forecast an ensemble of likely trajectories (time-series) of these key variables through 2050. These time-series, in turn, are used to generate recruitment trajectories, which are input into the stock projection model to examine likely responses of walleye pollock to climate-driven changes in recruitment, as well as to possible changes in predation from arrowtooth flounder (Figure 2).

**Methods**

Based on our current understanding of walleye pollock recruitment, a conceptual model of the most important factors determining the survival of early gadid stages, from spawning through recruitment at age 1, was developed, assuming that recruitment

variability occurs primarily at the larval and early juvenile stages. Suitable datasets for modelling the relationships between potential explanatory variables and survival of walleye pollock were selected to test the hypothesized mechanisms. Explanatory variables included timing of sea ice retreat and a spring transition index to capture conditions during the early larval stage; summer wind-mixing, late summer sea surface temperature (SST), and late summer water column stability to capture environmental conditions during the late larval stage; and an index of predation pressure on juvenile walleye pollock to estimate effects of the major predators, including cannibalism, on juvenile survival (Table 1).

**Modelling stock–recruitment residuals**

Because there is strong evidence of density-dependence in walleye pollock, residuals from a stock–recruitment (S–R) relationship were used as the primary response variable to quantify variability in survival. This index, also referred to as log-survival, removes the impact of spawning biomass on recruitment and should more accurately reflect the influence of environmental variability on

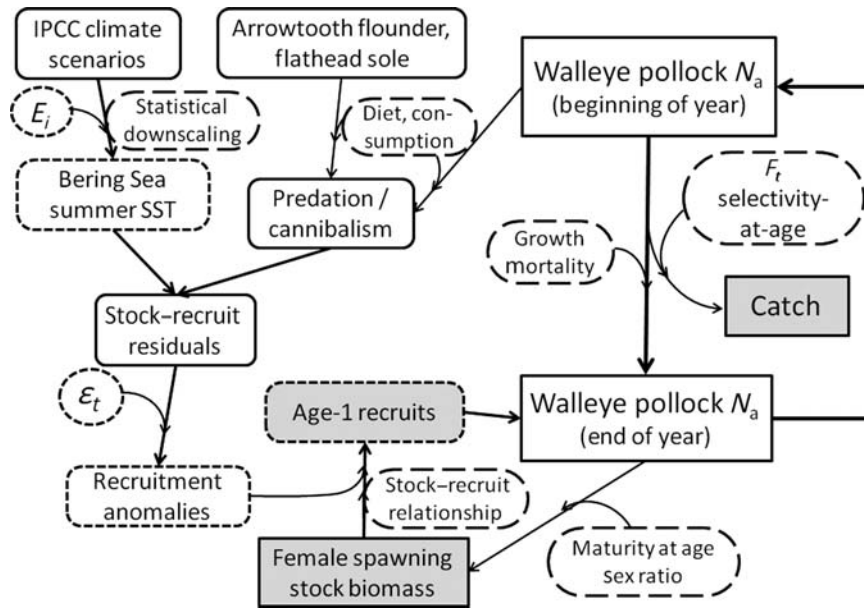


**Figure 2.** Flow chart of modelling and projection approach. Rectangles denote the main state variables of projection model (2009–2050), beginning with 2009 numbers-at-age ( $N_a$ ); long-dashed ovals denote the fixed input parameters ( $F_t$  is the annual fishing mortality based on the harvest control rule described in the text). Rounded rectangles denote inputs for the statistical regression model to generate future recruitment; short-dashed lines denote main stochastic elements generated by random draws from an ensemble of climate projections ( $E_i$ ) or from a specified distribution ( $\epsilon_t$ ). Shaded boxes denote quantities tracked and summarized in results.

**Table 1.** Pairwise Pearson’s correlation coefficients among independent variables used in analysis of walleye pollock recruitment with significance levels, and loadings of variables on first four PCs.

Variable	ICE	ST	SST	Wind	Strat	PC 1 (41%)	PC 2 (24%)	PC 3 (18%)	PC 4 (14%)
Ice retreat (ICE)						−0.48	0.27	0.35	<b>0.44</b>
Spring transition (ST)	0.77**					−0.59	0.09	0.11	0.24
Summer SST (SST)	−0.37**	−0.61**				<b>0.54</b>	0.15	0.21	<b>0.40</b>
Summer wind (Wind)	−0.19	−0.20	0.24			0.17	−0.65	0.12	<b>0.61</b>
Stratification (Str)	−0.03	−0.33*	0.59**	−0.32*		0.33	<b>0.66</b>	0.19	0.17
Predation (P)	0.04	−0.06	0.07	0.12	−0.04	0.04	−0.21	<b>0.87</b>	−0.43

Loadings larger than 0.4 are emboldened.

\* $p < 0.1$ .

\*\* $p < 0.05$ .

recruitment. The S–R relationship was estimated for year classes 1963–2008 within the 2009 age-structured assessment model (Ianelli *et al.*, 2009), using the following parametrization of the Ricker model:

$$R_t = \frac{SSB_{t-1}}{\emptyset_0} e^{\alpha(1-SSB_{t-1}/B_0)} e^{\varepsilon_t}, \quad (1)$$

where  $R_t$  is the recruitment at age 1 in year  $t$  at a given level of female spawning-stock biomass (SSB) and  $e^{\varepsilon_t}$  is a multiplicative error term. Parameters of the relationship were estimated to be  $\alpha = 2.084$ ,  $\emptyset_0 = 0.2631$ , and  $B_0 = 4934$  (Ianelli *et al.*, 2009). Although age-1 recruitment in the assessment model was estimated through 2008, relative year-class strength may be modified after the early juvenile stage, hence the estimate of the 2008 year class was deemed unreliable for this analysis.

Because of the large number of explanatory variables relative to the length of the available time-series and because of potential confounding among the variables, a principal components analysis (PCA) was used to reduce the number of explanatory variables to a smaller number of independent variables (PCs). To model recruitment or survival as a function of these PCs or as a function of individual variables, a generalized additive modelling approach (GAM), was used in the exploratory stages (Wood, 2006) and a general linear modelling approach was used for selecting the final model and for quantifying uncertainty for the projections. Therefore, S–R residuals ( $\varepsilon_t$ ) from Equation (1) were modelled as a function of one or more environmental variables acting in year  $t - 1$  ( $X_{i,t-1}$ ,  $i = 1, 2, \dots$ ), using an additive model with non-parametric smooth functions ( $f_i$ ) of the explanatory variables:

$$\varepsilon_t = \beta'_0 + f_1(X_{1,t-1}) + f_2(X_{2,t-1}) + \dots + \nu_t.$$

Potential interactions between the explanatory variables were also explored by fitting smooth functions (=smooth surfaces) of two environmental variables [e.g.  $f(X_1, X_2)$ ]. These interaction terms did not improve the models significantly and they were not considered further. The degree of smoothing was determined through generalized cross-validation (Wood, 2006); for the final models, smooth terms were replaced by linear or polynomial terms with approximately the same degrees of freedom as the estimated smooth terms:

$$\varepsilon_t = \beta_0 + \beta_1 X_{1,t-1} + \beta_2 X_{2,t-1} + \dots + \nu_t, \quad (2)$$

where the residuals  $\nu'_t$  or  $\nu_t$  are assumed to follow a normal distribution with variance  $\sigma_v^2$ ,  $\beta_0$  and  $\beta'_0$  the intercepts,  $\beta_1$  and  $\beta_2$  the slope parameters, and the  $X_i$  terms may be a quadratic or other power transformation of the measured variables. Residuals were tested for serial dependence and, if appropriate, residual variability was modelled as a first-order autoregressive process. The small sample or corrected Akaike Information Criterion (AIC<sub>c</sub>; Hurvich and Tsai, 1989) was used to identify the most parsimonious model for predicting recruitment. The estimated level of uncertainty in the identified relationships was incorporated in the projections as described below to characterize uncertainty in future population trajectories.

### Modelling recruitment

As an alternative to modelling S–R residuals estimated within the stock assessment model as a function of environmental variables,

recruitment estimates from the assessment were used in a “post-assessment” analysis as response variable in a generalized Ricker model (Quinn and Deriso, 1999). The linear form of this model describes log-transformed recruitment as a function of spawning biomass and environmental variables as follows:

$$\log(R_t) = \alpha + \beta SSB_{t-1} + \sum_i \gamma_i X_{i,t-1} + \log(SSB_{t-1}) + \varepsilon_t, \quad (3)$$

where  $\alpha$  and  $\beta$  are the productivity and carrying capacity parameters of the Ricker model, respectively, the  $X_i$  are one or more covariates acting on the egg and larval stages of walleye pollock before year  $t$ , the  $\gamma_i$  are the corresponding regression coefficients, and  $\varepsilon_t$  are either independent, normally distributed residuals, or follow a first-order autoregressive process. The second SSB term was included in the model as an offset without a coefficient. In the exploratory stage, we also fitted semi-parametric models with a linear term for SSB and smooth terms for the covariates  $X_i$ .

### Data sources

Long-term indices of environmental variability of potential importance to walleye pollock were constructed from various sources. Temperature indices were based on monthly extended reconstructed SSTs (ERSSTv3; Smith *et al.*, 2008), which are interpolated values on a 2° latitude × 2° longitude grid and were averaged over the southeast Bering Sea shelf inshore of the shelf break and extending to 61°N for this analysis. Monthly ERSST data were used to develop two indices of temperature conditions: a spring transition index related to the timing of the non-ice-associated spring phytoplankton bloom and a late summer SST index. The spring transition index was constructed by interpolating between monthly mean shelf temperatures (assumed to reflect temperatures on the 15th of each month) using a cubic spline and estimating the day of the year when smoothed temperatures first exceeded 4°C. As an index of late summer upper layer temperature conditions, the monthly ERSSTs were averaged over the southeast Bering Sea shelf from July 1 to September 30.

An index of the timing of sea ice retreat (ICE) for the period 1972–2003 was based on Palmer (2003), as described in Mueter *et al.* (2006), and was extended through 2008 using a regression-based proxy. The original index was defined as the International Organization for Standardization (ISO) week when average ice concentration in the National Marine Fisheries Survey (NMFS) area first drops below 20%, where ice concentrations were obtained from digital ice charts provided by the Arctic Climatology Project, National Ice Center, NOAA (<http://www.natice.noaa.gov>). Predicted values of the index for 2004–2008 were obtained from a multiple linear regression of the original index on mean April air temperatures at St Paul airport (57.15°N 170.22°W), mean April–May SST (ERSSTv3 averaged over the southeast Bering Sea shelf as described above), and the mean February through April north–south windspeed component at 10 m height near 56.2°N 168.75°W from the NCEP reanalysis (Kalnay *et al.*, 1996). The best-fit linear regression explained 90% of the variability in the observed ice retreat and predicted values were obtained as follows:

$$\begin{aligned} \text{ICE} = & 19.196 - 1.672 \times \text{SST} - 7.020 \times \nu - 2.346 \times \nu^2 - 3.329 \\ & \times \text{airT} - 2.504 \times \text{airT}^2 - 2.187 \times \text{airT}^3, \end{aligned}$$

where SST, airT, and  $\nu$  are the SST index, air temperature index, and N–S winds, respectively, as described above. The best regression model was determined by first finding the additive model with smooth terms for each variable that resulted in the best leave-one-out predictions (Wood, 2006), then substituting quadratic and cubic polynomial terms for smooth terms that had  $\sim 2$  and 3 degrees of freedom, respectively. The parametric fit was almost identical with the additive smooth fit and was chosen for the analysis to simplify the computation of predicted values and to enhance transparency.

To capture summer stratification, two alternative approaches were used. Data from a mooring at station M2 on the middle shelf for 1996–2007 (Stabeno *et al.*, 2001, 2007) were used to compute an index of water column stability during late summer. The stability index was computed as the negative depth-integrated potential energy ( $\text{J m}^{-2}$ ), or the energy required to mix the water column, following Simpson *et al.* (1977). Daily average temperature and salinity profiles at M2 were estimated from discrete depth measurements by linearly interpolating between consecutive depths before computing the stability index. Daily indices of stability were averaged from 1 July through 30 September. Because the measured time-series of stratification was much shorter than the recruitment series, a proxy for water column stability based on a one-dimensional model of mixed-layer depth was used to extend the time-series back to 1963 (C. Ladd, NOAA-PMEL, Seattle, pers. comm.). To quantify predation pressure, the only biotic variable in our analyses, diet compositions and consumption estimates from the early 1990s (Aydin *et al.*, 2007) were used to construct an index of “potential predation pressure”. The major sources of mortality for juvenile walleye pollock in the early 1990s, accounting for well more than 50% of the overall mortality, were adult walleye pollock, arrowtooth flounder, and flathead sole (Aydin *et al.*, 2007). Therefore, an index of predation in year  $t$  ( $\text{pred}_t$ ) was computed as follows:

$$\text{pred}_t = \sum_{i=1}^3 \left( \frac{Q}{B} \right)_i \times B_{i,t} \times p_i,$$

where  $(Q/B)_i$  is the consumption rate (consumption  $Q$  per unit biomass  $B$ ) of predator  $i$ ,  $B_{i,t}$  the estimated total biomass of predator  $i$  in year  $t$  (obtained from NPFMC, 2009), and  $p_i$  the average proportion of juvenile pollock in the diet of predator  $i$ . This assumes that both the consumption rate and the proportion of pollock in a predator diet remain the same as those estimated for the early 1990s. Clearly, both assumptions may be violated, because the consumption rate is a function of the age structure of the population and diet composition varies with the relative abundance of different prey, the spatial overlap of predators and prey, and other factors that affect prey availability. Therefore, potential effects of changes in spatial distribution of predators on pollock recruitment, as quantified by the centre of gravity, were examined, but were not significant and are not considered further here. The index of predation was computed across the three major predators from 1977 to 2008, when biomass estimates for all three species were available, and it was strongly correlated with the biomass of walleye pollock over this period ( $r = 0.91$ ), because adult walleye pollock are the main predators on juvenile pollock because of their large biomass. Therefore, we also correlated pollock S–R residuals with the biomasses of each individual predator to confirm the negative relationship between the biomass

of each predator and survival of walleye pollock from spawning to recruitment. Only arrowtooth flounder and flathead sole were included in the generalized Ricker model [Equation (3)], because cannibalism by walleye pollock is implicitly captured by the density-dependent term in this formulation (effect of SSB on log-recruitment).

### Regional temperature forecasts

To predict future recruitment of walleye pollock from global climate scenarios, regional forecasts of key environmental variables that drive recruitment variability of walleye pollock in the eastern Bering Sea are needed (Hollowed *et al.*, 2009). A statistical down-scaling approach was employed to forecast these variables, in particular summer SST over the shelf, from IPCC model projections. Because there are large uncertainties about any climate projection, 82 climate scenarios were considered to reflect the range of uncertainty in outcomes. Plausible future temperature scenarios to characterize the range of uncertainty were selected, based on a subset of nine IPCC models that performed best in capturing historical climate variability of the North Pacific in their 20th century hindcast simulations (Overland and Wang, 2007). It is assumed that the models that can replicate the observed spatial and temporal characteristics of the Pacific Decadal Oscillation are apt to be those that better handle the atmospheric forcing, air–sea interactions, and upper-ocean circulations of the North Pacific, including the Bering Sea, and that these models are therefore more reliable for simulations for the 21st century. Conversely, the evaluation of model skill is hampered by the existence of only one realization of the past climate and, therefore, it seems sensible to retain a relatively large number of individual models for producing a meaningful ensemble mean and quantifying future uncertainties. For the nine models chosen, 21st century projections with the low (B1), intermediate (A1B), and high (A2) CO<sub>2</sub> emissions scenarios were considered. All three scenarios were evaluated, because they span a wide range of simulated future climate forcing of the Bering Sea. In our use of IPCC climate model output, we have essentially followed the “best practices” outlined by Overland *et al.* (in press).

### Stock projections

Future recruitment series for walleye pollock were simulated under different climate scenarios and were used to drive a population dynamics model to explore the effects of climate variability on future population trajectories (Figure 2). Walleye pollock population numbers, biomass, and catches through 2050 were projected starting with the 2009 numbers-at-age as estimated in the most recent stock assessment (Ianelli *et al.*, 2009). To convert numbers to biomass, weights-at-age for all future years were assumed equal to the 1999–2008 observed average. Other parameter values for the projections were set equal to the values estimated by or used in Ianelli *et al.* (2009), including maturity-at-age, selectivity-at-age, and natural mortality. Projections used standard population dynamics equations as described in Ianelli *et al.* (2009) and a harvest control rule similar to the Tier 3 control rule used for many groundfish species off Alaska (NPFMC, 2002), but with an annual cap on total catches of  $1.5 \times 10^6$  t. This cap is close to recent maximum catches that have been achieved under the regulatory cap of  $2 \times 10^6$  t on total groundfish removals from the eastern Bering Sea, as specified in the Fishery Management Plan (NPFMC, 2002).

Because our focus was on exploring the effects of future climate changes on recruitment, all population parameters except recruitment were fixed in the simulations. This included reference points used in the harvest control rule, which are the unfished level of SSB ( $B_{100\%}$ , the projected spawning biomass under no fishing and assuming average recruitment based on the 1977–2008 period) and the corresponding fishing mortality rate ( $F_{40\%}$ ) that would reduce spawning biomass to 40% of the unfished biomass ( $B_{40\%}$ ). Under the assumed harvest control rule, the stock is fished at  $F_{40\%}$  if current biomass ( $B$ ) is larger than  $B_{40\%}$  and fishing is reduced linearly if the biomass declines below  $B_{40\%}$ . Moreover,  $F$  is set to zero if the biomass declines below 20% of the unfished biomass, as a precautionary measure that was implemented to protect the prey base for endangered Steller sea lions (*Eumetopias jubatus*).

Recruitment at age 1 was simulated for each year of the projections using one of the three general approaches:

- (i) *Random stock–recruitment residuals*: As a control and for comparisons with scenarios that include environmental effects on recruitment, we generated future recruitment series by randomly drawing values from the observed S–R residuals for brood years 1977–2007 [ $\varepsilon_t$  in Equation (1)] and calculating recruitment in year  $t$  according to Equation (1).
- (ii) *Simulated stock–recruitment residuals (type 1 model)*: Future S–R residuals under a given climate scenario were simulated from the  $AIC_c$  best model(s) for describing the climate–recruitment relationship [Equation (2)]. Values for  $\varepsilon_t$  in Equation (2) ( $\varepsilon_t^*$ ) were simulated by accounting for the full prediction uncertainty (i.e. parameter uncertainty plus residual uncertainty):

$$\varepsilon_t^* = \beta_0 + \beta_1 X_{1,t-1} + \beta_2 X_{2,t-1} + \dots + t_{df} \sqrt{\sigma_\beta^2 + \sigma_v^2},$$

where  $t_{df}$  is drawn from a Student's  $t$ -distribution with degrees of freedom equal to residual degrees of freedom of the best environmental model,  $\sigma_\beta^2$  is the variance of the predicted value at the given level of the environmental variables, and  $\sigma_v^2$  is the residual variance.

- (iii) *Simulated recruitment from the generalized Ricker model (type 2)*: Future recruitments were simulated from a lognormal distribution with predicted means and variances estimated from the  $AIC_c$  best model(s) of the form described in Equation (3).

The  $AIC_c$  best models in both cases (types 1 and 2) included predation terms. For type 1 models, the predation index was annually updated in the projections to account for changes in walleye pollock biomass, whereas arrowtooth flounder biomass and flat-head sole biomass were held constant at their 2009 values. Under type 2 models, two future scenarios were explored for arrowtooth flounder, assuming either a constant biomass at the 2009 value for all future years (model 2a) or a continuing linear increase in arrowtooth flounder biomass at the rate observed between 1991 and 2009 (model 2b).

## Results

Walleye pollock recruitment has undergone large fluctuations over recent decades (Figure 3). Large year classes tend to occur every 4–6

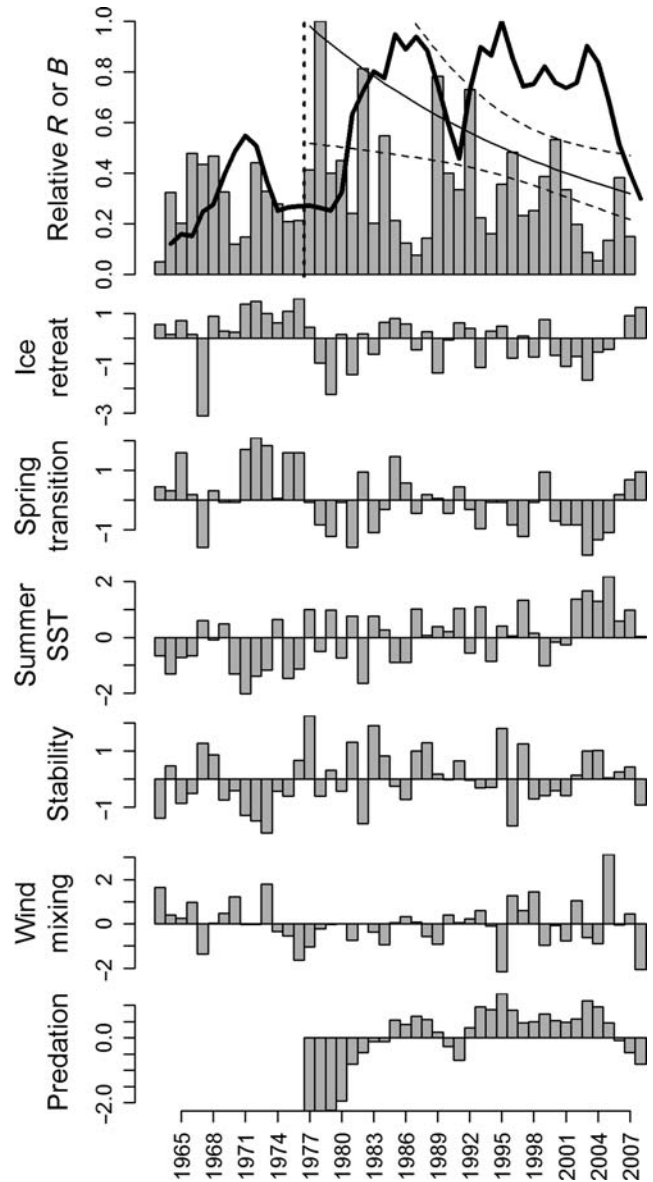


**Figure 3.** Time-series of walleye pollock recruitment (bars) and biomass (solid line) in the eastern Bering Sea, 1963–2009, based on most recent stock assessment estimates (lanelli *et al.*, 2009) and anomaly time-series of environmental variables used in the analysis. The vertical dashed line in the top panel denotes 1976/1977 climate regime shift. Thin line and thin dashed lines in the top panel indicate estimated 80th percentile of recruitment from 1977 to 2007, with 95% coverage interval based on a quantile regression of log-transformed recruitment over time ( $t = 2.57$ ,  $p = 0.015$ ).

years and can cause considerable fluctuations in biomass. Similar to other fish species in the Bering Sea (Mueter *et al.*, 2007), strong recruitment after the 1976/1977 climate regime shift resulted in a strong increase in biomass. The average estimated recruitment at age 1 was similar before (18.3 billion) and following the regime shift (22.3 billion,  $t$ -test on log-transformed abundances:  $t = -0.56$ ,  $p = 0.58$ ). However, several strong year classes originated after the regime shift starting in 1977, followed by a significant decrease in average log-transformed recruitment (linear trend over time:  $t = -2.24$ ,  $p = 0.033$ ). In particular, there has been a

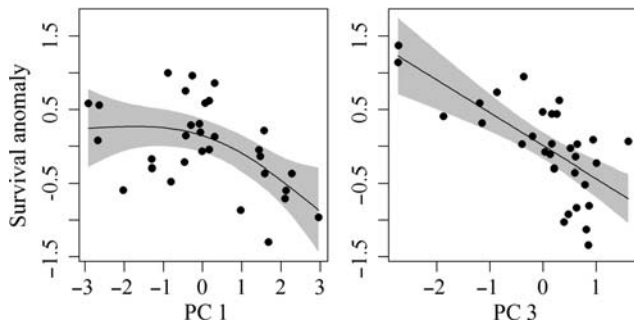


**Figure 4.** Predicted stock–recruitment residuals for walleye pollock in the eastern Bering Sea as a function of the first and the third PCs from a PCA of six environmental indicators. PC 1 reflects average temperature conditions, whereas PC 3 reflects predation pressure. Other PCs were not significant. Note that temperature and ice conditions in spring are confounded with summer temperature conditions and their apparent effects on recruitment cannot be separated statistically.

considerable decrease in the strength of the largest year classes. For example, a quantile regression reveals a significant decrease in the 80th percentile of log-transformed recruitment over time (Figure 3, top panel).

Environmental variables were characterized by high interannual variability over most of the time-series, with a few multiyear periods of consistent cold (1971–1976) or warm (2001–2005) conditions (Figure 3). As expected, temperature, ice, and spring transition indices were correlated with each other and, to a lesser extent, with the stratification index (Table 1). Importantly, the predation index was not correlated with any of the environmental indices.

Correlations between environmental variables were used to reduce the number of variables to four significant PCs, which accounted for 97% of the overall variability (Table 1). The first PC contrasts warm years characterized by little ice, an early spring transition, and warm summer SST with cold years. Warm years tend also to be strongly stratified (positive loading for stratification index). However, variability in stratification and wind-mixing are primarily captured by PC 2, which contrasts years characterized by weak wind-mixing and strong stratification (positive values of PC 2) with years that have strong wind-mixing and weak stratification (negative PC 2). The third PC primarily reflects predation with weak loadings on all the environmental variables, whereas PC 4 in its positive phase was associated with unusual years characterized by both a late ice retreat and warm summers with strong wind-mixing.

### Recruitment modelling

For models of type 1, the best overall model based on  $AIC_c$  explained much of the variability in S–R residuals (adjusted  $r^2 = 0.55$ ; Figure 4) as a function of PC 1 (smooth fit with  $\sim 2$  d.f.,  $F = 5.36$ ,  $p = 0.0088$ ) and PC 3 (linear term,  $F = 25.5$ ,  $p < 0.001$ ). Neither PC 2 nor PC 4 was significantly related to variability in S–R residuals, and there was no significant interaction between PC 1 and any of the other PCs. Therefore, variability in survival appears to be most strongly related to overall temperature variability (PC 1) and predation (PC 3), and survival anomalies were highest when temperatures were low to intermediate and when the predation index was low to average (Figure 4). Because

of strong correlations between the variables (Table 1), the relative effects of spring and summer conditions on survival cannot be separated statistically. However, GAMs of S–R residuals as a function of individual variables suggest that survival was significantly related to late summer SST (3 d.f., adjusted  $r^2 = 0.24$ ,  $F = 4.46$ ,  $p = 0.0082$ ), but not to the timing of the ice retreat ( $p = 0.775$ ) or to the spring transition index ( $p = 0.382$ ). Therefore, late summer SST appears to be more important in determining survival to recruitment than spring ice and temperature conditions.

To predict future survival anomalies (S–R residuals) from available climate forecasts, the model was simplified further. First, we replaced PC 1 in the model with average July–September SSTs, because ice conditions and the spring transition index were not significant individually and because ice retreat is difficult to forecast from current climate models. Second, we replaced the smooth terms with a quadratic term for SST and a linear term for predation to fit a linear regression model. The resulting model provided a reasonable fit (Figure 5, adjusted  $r^2 = 0.46$ ,  $F = 9.51$ ,  $p < 0.001$ ) and will be referred to as model 1 in the projections. Further model comparisons confirmed that none of the other variables improved the model significantly when added individually ( $AIC_c$  always increased) and that there was no significant interaction between SST and predation (difference in  $AIC_c$  values:  $\Delta AIC_c = 4.5$ ). Residuals from the best model were not significantly autocorrelated (Durbin–Watson test statistic = 1.82,  $p = 0.243$ ) and were close to normally distributed (Shapiro–Wilk test for normality,  $W = 0.968$ ,  $p = 0.471$ ). Although walleye pollock dominated the predation term in the model, the biomass of each individual predator had a negative effect on S–R residuals at the 90% significance level (walleye pollock:  $p < 0.001$ ; arrowtooth flounder:  $p = 0.014$ ; flathead sole:  $p = 0.065$ ).

An alternative model of type 2, using recruitment and spawner biomass estimates from the stock assessment to fit a generalized Ricker model, suggested similar significant effects of late summer temperatures on log-transformed recruitment. An exploratory model with a smooth term for summer SST suggested that (log-) recruitment was relatively high at lower SSTs, dropped steeply between  $\sim 9.2$  and  $9.8^\circ\text{C}$  and was low at higher temperatures. We therefore replaced the smooth term for SST with a threshold at  $9.4^\circ\text{C}$ , where the threshold value was estimated within the model (Figure 5). The biomass of arrowtooth flounder was related significantly and negatively to pollock recruitment (simple linear regression,  $t = -2.115$ ,  $p = 0.043$ ), but the effect was not significant when arrowtooth flounder was included in the generalized Ricker model ( $p = 0.106$ ). Nevertheless, a negative coefficient is consistent with a predation effect and with the model described above; hence, arrowtooth flounder biomass was included in the model to examine the possible effects of different future arrowtooth trajectories on pollock recruitment (Figure 5, adjusted  $r^2 = 0.56$ ,  $F = 13.9$ ,  $p < 0.001$ ). This model is referred to as model 2 in the projections.

### Projections

Ensemble predictions of future trajectories for average July–September SST under three emissions scenarios display very high variability in individual trajectories and a gradual increase in the ensemble mean through 2050 (Figure 6). On average, late summer SSTs in the eastern Bering Sea are expected to increase by  $\sim 1^\circ\text{C}$  under IPCC emissions scenarios A2 and B1 and a somewhat larger increase under scenario A1B. The larger increase in the

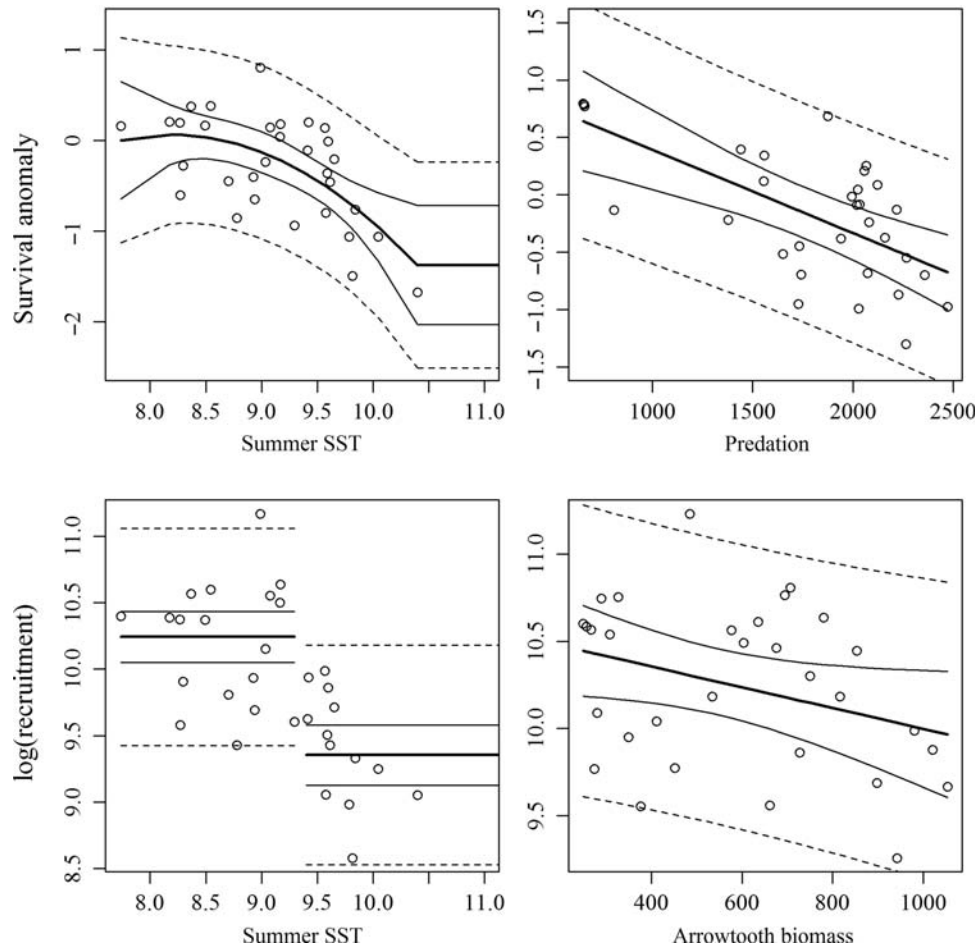


**Figure 5.** Estimated effects of summer (July–September) SST and combined predation by walleye pollock, arrowtooth flounder, and flathead sole on survival anomalies (stock–recruitment residuals) of walleye pollock (top panels) and estimated effects of summer SST and arrowtooth flounder biomass on log-transformed recruitment (density-dependent effect of spawning biomass not illustrated).

A1B scenario can be attributed to slightly faster growth in global temperatures relative to the higher emissions A2 scenario until approximately ~2050 (at which point temperatures under the A2 scenario begin to increase at a greater rate) and perhaps to a regional effect.

Simulated population trajectories of walleye pollock were highly variable, because of large variability in recruitment resulting from high variability in future SST trajectories and large uncertainties in the estimated effects of SST and predation (Figure 7). Under model 1, average recruitment across the three emissions scenarios is expected to decline over the next 40 years by ~44% relative to the random recruitment scenario (based on 1977–2007 mean, see Figures 7 and 8). However, a 90% simulation envelope includes the 1977–2007 mean, implying approximately a 13% probability that average recruitment will be higher than the 1977–2007 mean in 2050. Similarly, spawning biomass and catches are expected to decline substantially with less than a 7.5% probability that spawning biomass will exceed  $B_{40\%}$  in 2050. Many of the catch trajectories resulted in zero catches during later years under model 1, because of the spawning biomass frequently falling below the  $B_{20\%}$  threshold (Figure 7).

The expected distribution of recruitment, spawner biomass, and catches are expected to decrease relative to the random recruitment scenario under both models (types 1 and 2) and

with (2b) or without (2a) a continuing increase in arrowtooth flounder biomass (Figure 8). The simulated values had a similar distribution under all three emission scenarios, with slightly larger declines under scenario A1B. Declines under model 2a were moderate, because of a strong compensatory response in recruitment implied by the generalized Ricker model (i.e. recruitment increases considerably, on average, at lower levels of SSB). If arrowtooth flounder biomass continues to increase, as assumed under model 2b, recruitment, spawner biomass, and catches are expected to decrease substantially relative to the random recruitment scenario and relative to the model that assumes that arrowtooth flounder biomass remains at the current level (Figure 8).

### Discussion

Empirical relationships between SSTs on the southeastern Bering Sea shelf during late summer and recruitment success of walleye pollock suggest that recruitment is reduced if regional average surface temperatures exceed ~9.4°C. The implications of these findings are that increasing temperatures in the eastern Bering Sea, as predicted by IPCC climate models under a range of scenarios (Figure 6), will likely reduce future recruitment, biomass, and harvests of walleye pollock (Figure 8). However, large



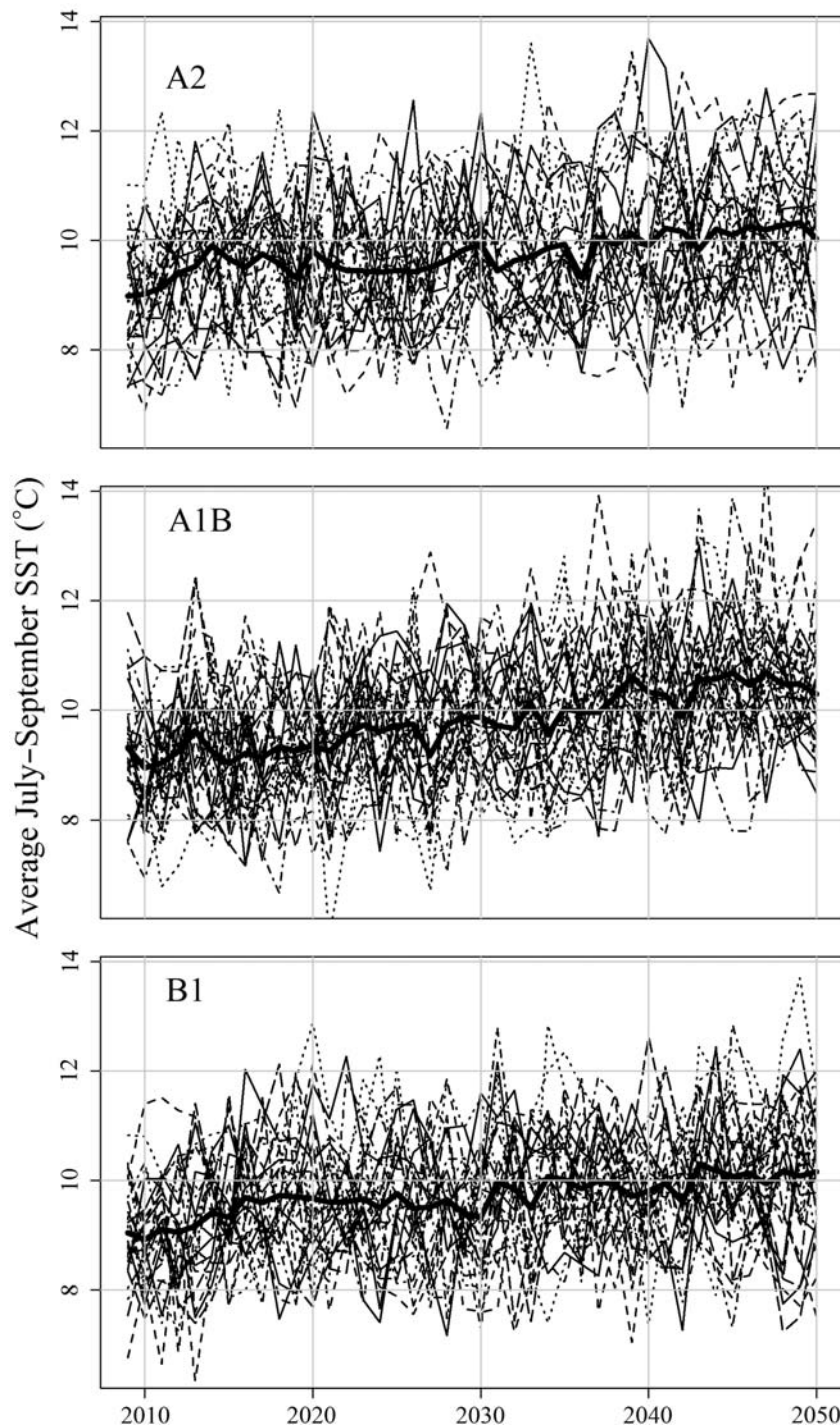


**Figure 6.** Ensemble predictions for late summer (July–September) SST through 2050 based on three IPCC climate scenarios.

uncertainties in SST projections and in the estimated relationships result in large uncertainties in future population trajectories. Under the assumed harvest scenario, there is large overlap in simulated trajectories between the random recruitment scenario and all the temperature-dependent scenarios, but under all models, there is a very high probability that future biomass and catches will be lower than in the past. Simulations under a variety of plausible future management scenarios result in similar conclusions (Ianelli *et al.*, 2011).

#### Environmental effects on recruitment

Our results are consistent with recent findings that unusually warm conditions during the period from 2002 to 2005 resulted in poor feeding conditions and low energy content of age-0 pollock in autumn months (Coyle *et al.*, 2011; Hunt *et al.*, 2011). Despite large abundances of age-0 pollock in surface waters during those years (Moss *et al.*, 2009), the survival of the 2002–2005 year classes was low and resulted in very poor recruitment (Figure 3), presumably as a consequence of reduced

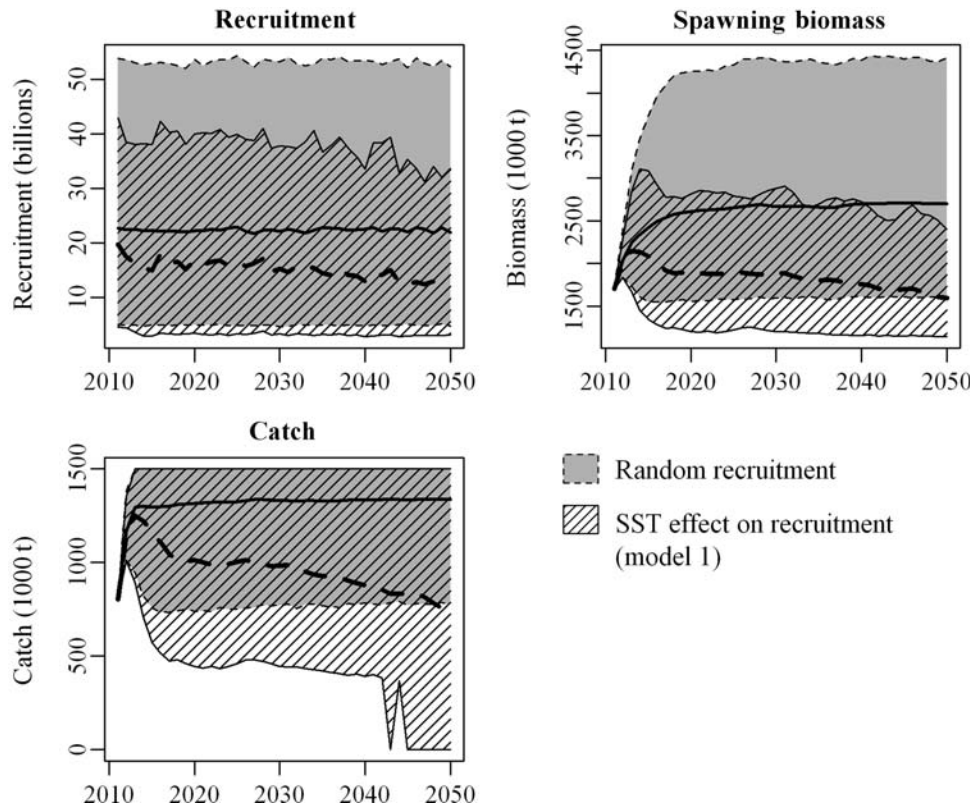


**Figure 7.** Distribution of simulated recruitment, spawning biomass, and annual catches for 2011–2050 under a model with no temperature effect (i.e. random recruitment) and under a model incorporating SST and predation effects on recruitment (model 1). Thick lines indicate means over 1000 simulated trajectories under random recruitment (solid line) and under model 1 (dashed line). Polygons denote simulation envelopes such that 90% of simulated values fall within the envelope in any given year. Future SST trajectories for these simulations were drawn at random from all the trajectories in Figure 6.

overwinter survival from age 0 to age 1 (Hunt *et al.*, 2011). Poor feeding conditions during the warm period resulted from a lack of large *Calanus* copepods, euphausiids (in particular *Thysanoessa raschii*), and other large zooplankton species that are important prey for larval and early juvenile pollock. The mechanisms that caused low abundances of large *Calanus* copepods and other large zooplankton are understood poorly and may relate to a mismatch between the timing of the spring bloom and the prey needs of copepod nauplii (Baier and Napp, 2003; Hunt *et al.*, 2011), or to a reduction in post-bloom production resulting from intense stratification and reduced nutrient supply into the surface layer (Coyle *et al.*, 2008, 2011; Hunt *et al.*, 2008). The latter hypothesis implies that reduced summer productivity limits food availability, growth, and subsequent survival of large zooplankton and may cause them to descend into deeper waters earlier in the season compared with cold years. Our results support the importance of late summer and autumn conditions, but strong confounding between spring and summer temperature conditions (Table 1) do not allow us to separate these non-exclusive hypotheses statistically.

Several studies provide evidence of the importance of upper-layer temperatures and water-column stratification, particularly during late summer and autumn, for the survival of young-of-year walleye pollock. There was a very strong and negative correlation between a measure of water column stratification at the M2 mooring site during July–September and pollock survival (1996–2007,  $r = -0.86$ ,  $p < 0.001$ ; Coyle *et al.*, 2011), although

this relationship became non-significant when the extended, model-based index of water-column stratification (Figure 3) was used as a proxy for conditions at M2 (FJM, unpublished data). This may indicate that the index is a poor measure of stratification in earlier years, that the importance of stratification has increased in recent years, or that the relationship is a result of other factors associated with stratification. Strong stratification during warm years generally implies a shallower thermocline and a thinner upper layer. This may result in food limitations, because of the reduction in available habitat and increased energetic demands because of warmer temperatures (Ciannelli *et al.*, 1998). Similarly, during years with warm temperatures in autumn, walleye pollock in the Gulf of Alaska may suffer from higher predation and limited food availability (Ciannelli *et al.*, 2004). Temperatures and stratification on the eastern Bering Sea shelf are weakly correlated (Table 1) and warm years (e.g. 2000 and 2001) can have low stratification, whereas cold years, such as 2007, can have very high stratification (C. Ladd, pers. comm.), providing some contrast between temperature and stratification. Results from the PCA suggest, to the extent effects can be disentangled, that temperature conditions (PC 1; Table 1) are more important than stratification (PC 2) to pollock survival.

The finding that warm conditions in the eastern Bering Sea are associated with poor survival contradicts earlier findings that warmer years tend to produce strong year classes of walleye pollock (Quinn and Niebauer, 1995; Hollowed *et al.*, 2001; Mueter *et al.*, 2006). This apparent contradiction can be resolved

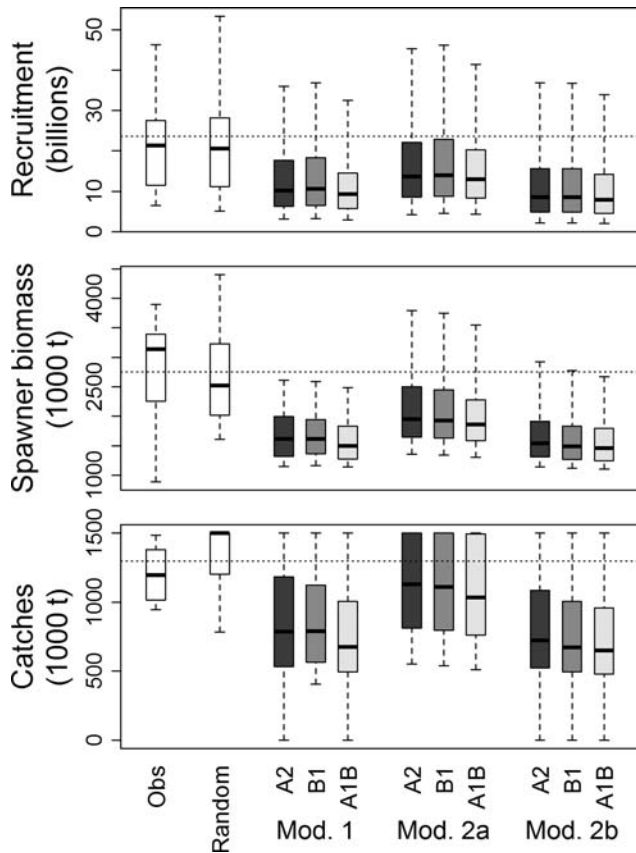


**Figure 8.** Boxplots of recruitment, spawner biomass, and catches as observed in the past (1979–2008, Obs) and as projected into the future (2041–2050 averages) using different models and climate scenarios. Boxes labelled “Random” assume no climate effect on recruitment (random draws from the observed values). Other boxes illustrate distribution of projected values under three different models to simulate temperature and predation effects on recruitment (see text for model details) and under three different IPCC emission scenarios. Dashed horizontal reference lines denote the mean values from “Random” scenario, black bars denote the median, boxes include central 50%, and whiskers include central 90% of simulated values. Note that the implemented harvest control rule limits catches to  $1.5 \times 10^6$  t, hence median, upper quartile, and upper whisker all coincide in some cases.

by observing that warmer springs with an early ice retreat appear to favour survival of early larvae (Hunt et al., 2011), but excessive warm temperatures in the autumn result in poor overwinter survival, resulting in a dome-shaped relationship between pollock survival and SST. The current analysis was limited to the post-regime shift period when SSTs were near the “optimum” SST range or on the descending limb of the hypothesized relationship (Figure 5). However, a dome-shaped relationship is evident if the full time-series of pollock recruitment (1963–2007) is plotted against late summer SST (Figure 9 in Coyle et al., 2011). Similarly, Pacific cod (*Gadus macrocephalus*), whose recruitment is strongly correlated with that of walleye pollock in the eastern Bering Sea, switched from a positive relationship between SST and recruitment before the 1976/1977 regime shift to a negative relationship after the regime shift (Mueter et al., 2009), when average temperatures were higher.

The projections presented here assume that the mechanisms that caused low recruitment during the recent warm period, which were followed by a dramatic decline in pollock biomass, will continue to operate into the future. Although such empirical relationships frequently break down over time (Myers, 1998), recent field observations, spanning a period of contrasting warm and cold conditions, offer strong support for a decrease in recruitment under very warm conditions (Hunt et al., 2011). This support is based on a mechanistic understanding of variability in prey conditions affecting pollock survival; hence, we believe that the estimated SST effect offers a reasonable basis for simulating future recruitment variability, as long as the associated uncertainties are taken into account.

### Uncertainties in stock projections

In this study, we only considered uncertainty in future SST trajectories and in the relationship between SST and recruitment as estimated outside the assessment. Clearly, the population dynamics of walleye pollock are highly uncertain and future improvements should consider full uncertainty in the assessment and in the estimated management parameters. Moreover, the estimation of SST effects could be integrated within the assessment model for consistency between the retrospective estimation and future projections. Additional uncertainties about the effect of SST on future recruitment arise from extrapolating the estimated SST relationship beyond the range of observed temperatures. Projections of late summer SST used in this study exceed the maximum observed value ( $10.4^\circ\text{C}$ )  $\sim 29\%$  of the time, with temperatures under some scenarios exceeding  $13.5^\circ\text{C}$  in individual years. It is assumed here that recruitment is not further reduced when SST exceeds the observed maximum (Figure 5), an assumption that is likely to underestimate the true effect of climate warming on recruitment. However, prey and/or pollock dynamics could change fundamentally under continued warming, for example, through northward shifts in the distribution of spawning and nursery areas. Such adaptive responses cannot be predicted currently, but populations may be particularly vulnerable during the periods of adaptation or the rate of change may overwhelm the ability of species to adapt (Brander, 2010), implying a need for additional precaution under rapid climate change.

Additional uncertainties in the projections arise from the incorporation of density-dependent effects (including cannibalism) and predation in models of recruitment. The stock–recruitment relationship estimated within the stock assessment model implies a moderate level of density-dependence (Ianelli et al., 2009). The effect of density-dependence can be evaluated by comparing changes in recruitment under models with and without density-dependence and by comparing models with different levels of density-dependence. The projections of Ianelli et al. (2011) predicted future (log-transformed) recruitment directly from SST, without taking account of density-dependence or predation. This is comparable with recruitment predictions from model 1, which included density-dependence, if predation is fixed at the observed mean. Results (not given) suggest relatively minor differences in recruitment projections under this level of density-dependence. In contrast, a generalized Ricker model fit to the assessment output implies a higher level of density-dependence, resulting in strong compensatory increases in recruitment at low levels of SSB, thereby moderating the influence of declining SST on recruitment (model 2a in Figure 8).

Strong density-dependence in the generalized Ricker model may be a consequence of within-cohort competition, within-cohort cannibalism, and cannibalism by adult pollock. Cannibalism is a major source of pollock mortality in the Bering Sea (Dwyer *et al.*, 1987; Livingston and Lang, 1996); it was evident in the effect of the predation term in model 1 and was a likely reason for the strong density-dependence in model 2. Predation by arrowtooth flounder, a major predator on juvenile pollock (Aydin *et al.*, 2007), also had a strong impact on future pollock dynamics. Arrowtooth flounder predation is believed to play a major role in regulating recruitment of walleye pollock in the Gulf of Alaska (Bailey, 2000; Hollowed *et al.*, 2000) and our results suggest that a continued increase in arrowtooth flounder biomass in the eastern Bering Sea could have a strong impact on pollock recruitment (Figure 8).

## Conclusions

Forecasts of the recruitment response of walleye pollock to future climate variability can be used within a management-strategy evaluation framework to assess alternative harvest scenarios and to provide long-term strategic advice to managers who are confronted with a rapidly changing environment (Ianelli *et al.*, 2011). This study only considered the effects of temperature and major groundfish predators on recruitment as a first step in assessing the effects of climate change on a major commercial species in the Bering Sea. Efforts are currently underway as part of the BEST/BSIERP research programme ([www.bsierp.nprb.org](http://www.bsierp.nprb.org)) to develop an end-to-end model of the eastern Bering Sea for predicting the responses of a multispecies fish community to future climate variability, but the model is not yet operational (K. Aydin, NOAA-AFSC, Seattle, pers. comm.). In the near term, studies such as this and Ianelli *et al.* (2011) in the Bering Sea and a similar study in the Baltic Sea (ICES 2009; A. Gårdmark, Swedish Board of Fisheries, pers. comm.) are likely to provide the best assessment of climate effects on single species as a basis for providing relevant management advice. These studies could be extended to include other effects of climate change, such as effects on growth and distribution, but are inadequate for capturing multispecies interactions or adaptive responses to warming.

## Acknowledgements

NOAA ERSST v3 data, air temperatures at St Paul airport, and NCEP Reanalysis data were provided by the NOAA/OAR/ESRL PSD, Boulder, CO, USA, from their website at <http://www.esrl.noaa.gov/psd/>. We thank our colleagues in the BEST-BSIERP Project, which is supported by NSF and NPRB, for many valuable discussions and access to data and manuscripts. In particular, we thank Phyllis Stabeno for providing the M2 data, Carol Ladd for providing the stratification index, Robert Lauth for providing bottom-trawl survey data for Figure 1, and Ed Farley for providing BASIS survey data for age-0 distributions in Figure 1. This is NPRB contribution #287 and BEST-BSIERP contribution #18.

## References

Aydin, K., Gaichas, S., Ortiz, I., Kinzey, D., and Friday, N. 2007. A comparison of the Bering Sea, Gulf of Alaska, and Aleutian Islands large marine ecosystems through food web modeling. NOAA Technical Memorandum NMFS-AFSC-178. 298 pp.

Bacheler, N. M., Ciannelli, L., Bailey, K. M., and Duffy-Anderson, J. T. 2010. Spatial and temporal patterns of walleye pollock (*Theragra*

*chalcogramma*) spawning in the eastern Bering Sea inferred from egg and larval distributions. Fisheries Oceanography, 19: 107–120.

Baier, C. T., and Napp, J. M. 2003. Climate-induced variability in *Calanus marshallae* populations. Journal of Plankton Research, 25: 771–782.

Bailey, K. M. 2000. Shifting control of recruitment of walleye pollock *Theragra chalcogramma* after a major climatic and ecosystem change. Marine Ecology Progress Series, 198: 215–224.

Brander, K. 2010. Impacts of climate change on fisheries. Journal of Marine Systems, 79: 389–402.

Ciannelli, L., Brodeur, R. D., and Buckley, T. W. 1998. Development and application of a bioenergetics model for juvenile walleye pollock. Journal of Fish Biology, 52: 879–898.

Ciannelli, L., Chan, K-S., Bailey, K. M., and Stenseth, N. Ch. 2004. Nonadditive effects of the environment on the survival of a large marine fish population. Ecology, 85: 3418–3427.

Coyle, K. O., Eisner, B., Mueter, F. J., Pinchuk, A. I., Janout, M. A., Cieciel, K. D., Farley, E. V., *et al.* 2011. Climate change in the southeastern Bering Sea: impacts on pollock stocks and implications for the oscillating control hypothesis. Fisheries Oceanography, 20: 139–156.

Coyle, K. O., Pinchuk, A. I., Eisner, L. B., and Napp, J. M. 2008. Zooplankton species composition, abundance and biomass on the eastern Bering Sea shelf during summer: the potential role of water-column stability and nutrients in structuring the zooplankton community. Deep Sea Research II: Topical Studies in Oceanography, 55: 1775–1791.

Dwyer, D. A., Bailey, K. M., and Livingston, P. A. 1987. Feeding habits and daily ration of walleye pollock (*Theragra chalcogramma*) in the eastern Bering Sea, with special reference to cannibalism. Canadian Journal of Fisheries and Aquatic Sciences, 44: 1972–1984.

Hollowed, A. B., Bond, N. A., Wilderbuer, T. K., Stockhausen, W. T., A'mar, Z. T., Beamish, R. J., Overland, J. E., *et al.* 2009. A framework for modelling fish and shellfish responses to future climate change. ICES Journal of Marine Science, 66: 1584–1594.

Hollowed, A. B., Hare, S. R., and Wooster, W. S. 2001. Pacific basin climate variability and patterns of Northeast Pacific marine fish production. Progress in Oceanography, 49: 257–282.

Hollowed, A. B., Ianelli, J. N., and Livingston, P. A. 2000. Including predation mortality in stock assessments: a case study for Gulf of Alaska walleye pollock. ICES Journal of Marine Science, 57: 279–293.

Hunt, G. L., Coyle, K. O., Eisner, L. B., Farley, E. V., Heintz, R. A., Mueter, F., Napp, J. M., *et al.* 2011. Climate impacts on eastern Bering Sea food webs: a synthesis of new data and an assessment of the Oscillating Control Hypothesis. ICES Journal of Marine Science, 68: 1230–1243.

Hunt, G. L., Stabeno, P., Walters, G., Sinclair, E., Brodeur, R. D., Napp, J. M., and Bond, N. A. 2002. Climate change and control of the southeastern Bering Sea pelagic ecosystem. Deep Sea Research II: Topical Studies in Oceanography, 49: 5821–5853.

Hunt, G. L., Stabeno, P. J., Strom, S., and Napp, J. M. 2008. Patterns of spatial and temporal variation in the marine ecosystem of the southeastern Bering Sea, with special reference to the Pribilof Domain. Deep Sea Research II: Topical Studies in Oceanography, 55: 1919–1944.

Hurvich, C. M., and Tsai, C-L. 1989. Regression and time series model selection in small samples. Biometrika, 76: 297–307.

Ianelli, J. N., Hollowed, A. B., Haynie, A. C., Mueter, F. J., and Bond, N. A. 2011. Evaluating management strategies for eastern Bering Sea walleye pollock (*Theragra chalcogramma*) in a changing environment. ICES Journal of Marine Science, 68: 1297–1304.

Ianelli, J. N., Barbeaux, S., Honkalehto, T., Kotwicki, S., Aydin, K., and Williamson, N. 2009. Assessment of the walleye pollock stock in the eastern Bering Sea. In Stock Assessment and Fishery Evaluation Report for the Groundfish Resources of the Bering Sea/Aleutian

- Islands Regions. North Pacific Fishery Management Council, Anchorage, AK.
- ICES. 2009. Report of the ICES/HELCOM Working Group on Integrated Assessments of the Baltic Sea (WGIAB), Rostock, Germany, 16–20 March 2009. ICES Document CM 2009/BCC: 02. 80 pp.
- Kalnay, E., Kanamitsu, M., Kistler, R., Collins, W., Deaven, D., Gandin, L., Iredell, M., *et al.* 1996. The NCEP/NCAR 40-year reanalysis project. *Bulletin of the American Meteorological Society*, 77: 437–472.
- Kotwicki, S., Buckley, T. W., Honkalehto, T., and Walters, G. 2005. Variation in the distribution of walleye pollock (*Theragra chalcogramma*) with temperature and implications for seasonal migration. *Fishery Bulletin US*, 103: 574–587.
- Livingston, P. A., and Lang, G. M. 1996. Interdecadal comparisons of walleye pollock, *Theragra chalcogramma*, cannibalism in the eastern Bering Sea. NOAA Technical Report NMFS, 126. 115 pp.
- Moss, J. H., Farley, E. V., Feldman, A. M., and Ianelli, J. N. 2009. Spatial distribution, energetic status, and food habits of eastern Bering Sea age-0 walleye pollock. *Transactions of the American Fisheries Society*, 138: 497–505.
- Mueter, F. J., Boldt, J., Megrey, B. A., and Peterman, R. M. 2007. Recruitment and survival of Northeast Pacific Ocean fish stocks: temporal trends, covariation, and regime shifts. *Canadian Journal of Fisheries and Aquatic Sciences*, 64: 911–927.
- Mueter, F. J., Broms, C., Drinkwater, K. F., Friedland, K. D., Hare, J. A., Hunt, G. L., Melle, W., *et al.* 2009. Ecosystem responses to recent oceanographic variability in high-latitude northern hemisphere ecosystems. *Progress in Oceanography*, 81: 93–110.
- Mueter, F. J., Ladd, C., Palmer, M. C., and Norcross, B. L. 2006. Bottom-up and top-down controls of walleye pollock (*Theragra chalcogramma*) on the eastern Bering Sea shelf. *Progress in Oceanography*, 68: 152–183.
- Myers, R. A. 1998. When do environment-recruitment correlations work? *Reviews in Fish Biology and Fisheries*, 8: 285–305.
- NPFMC. 2002. Fishery Management Plan for the Bering Sea/Aleutian Islands Groundfish. North Pacific Fishery Management Council, 605 West 4th Avenue, Suite 306, Anchorage, AK 99501. 383 pp.
- NPFMC. 2009. Stock Assessment and Fishery Evaluation Report for the Groundfish Resources of the Bering Sea/Aleutian Islands Regions. North Pacific Fishery Management Council, 605 West 4th Avenue, Suite 306, Anchorage, AK 99501. 383 pp.
- Overland, J. E., and Wang, M. 2007. Future climate of the North Pacific Ocean. *EOS Transactions of the American Geophysical Union* 88: 178–182.
- Overland, J. E., Wang, M., Bond, N. A., Walsh, J. E., Kattsov, V. M., and Chapman, W. L. Considerations in the selection of global climate models for regional climate projections: the Arctic as a case study. *Journal of Climate* in press.
- Palmer, M. C. 2003. Environmental controls of fish growth in the southeast Bering Sea. Institute of Marine Science, University of Alaska Fairbanks. 60 pp.
- Quinn, T. J., and Deriso, R. B. 1999. *Quantitative Fish Dynamics*. Oxford University Press New York.
- Quinn, T. J., and Niebauer, H. J. 1995. Relation of eastern Bering Sea walleye pollock recruitment to environmental and oceanographic variables. *In Climate Change and Northern Fish Populations* pp. 497–507. Ed. by R. J. Beamish. National Research Council of Canada, Ottawa.
- Rijnsdorp, A. D., Peck, M. A., Engelhard, G. H., Möllmann, C., and Pinnegar, J. K. 2009. Resolving the effect of climate change on fish populations. *ICES Journal of Marine Science* 66: 1570–1583.
- Simpson, J. H., Hughes, D. G., and Morris, N. C. G. 1977. The relation of seasonal stratification to tidal mixing on the continental shelf. *Deep Sea Research*, 24: 327–339.
- Smith, T. M., Reynolds, R. W., Peterson, T. C., and Lawrimore, J. 2008. Improvements to NOAA's historical merged land-ocean surface temperature analysis (1880–2006). *Journal of Climate*, 21: 2283–2296.
- Stabeno, P. J., Bond, N. A., Kachel, N. B., Salo, S. A., and Schumacher, J. D. 2001. On the temporal variability of the physical environment over the south-eastern Bering Sea. *Fisheries Oceanography*, 10: 81–98.
- Stabeno, P. J., Bond, N. A., and Salo, S. A. 2007. On the recent warming of the southeastern Bering Sea shelf. *Deep Sea Research*, 54: 2599–2618.
- Wespestad, V. G., Fritz, L. W., Ingraham, W. J., and Megrey, B. A. 2000. On relationships between cannibalism, climate variability, physical transport, and recruitment success of Bering Sea walleye pollock (*Theragra chalcogramma*). *ICES Journal of Marine Science*, 57: 272–278.
- Wood, S. N. 2006. *Generalized Additive Models: an Introduction with R*. Chapman and Hall/CRC, Boca Raton, FL, USA.
- Wyllie-Echeverria, T. 1996. The relationship between the distribution of one-year-old walleye pollock, *Theragra chalcogramma*, and sea-ice characteristics. NOAA Technical Report NMFS, 126: 47–56.